ARTICLE

BIOTECHNOLOGY and BIOENGINEERING

Chip-Based Protein–Protein Interaction Studied by Atomic Force Microscopy

Feng-Sheng Kao,[1,2] Waylon Ger,[1,3] Yun-Ru Pan,[1] Hui-Chen Yu,[1] Ray-Quen Hsu,[2] Hueih-Min Chen[1]

[1]National Nano Device Laboratories, Nano Biomedical & MEMS Technology Division, No. 26, Prosperity Road I, Hsinchu Science Park, Hsinchu, Taiwan, telephone: +886-3-5726100 ext 7712, fax: +886-3-5726109; e-mail: hmchen@ndl.narl.org.tw

[2]Department of Mechanical Engineering, National Chiao Tung University, Hsinchu, Taiwan

[3]National Chiao Tung University, Institute of Physics, Hsinchu, Taiwan

ABSTRACT: In this article, a technique for accurate direct measurement of protein-to-protein interactions before and after the introduction of a drug candidate is developed using atomic force microscopy (AFM). The method is applied to known immunosuppressant drug candidate *Echinacea purpurea* derived cynarin. T-cell/CD28 is on-chip immobilized and B-cell/CD80 is immobilized on an AFM tip. The difference in unbinding force between these two proteins before and after the introduction of cynarin is measured. The method is described in detail including determination of the loading rates, maximum probability of bindings, and average unbinding forces. At an AFM loading rate of 1.44×10^4 pN/s, binding events were largely reduced from $61 \pm 5\%$ to $47 \pm 6\%$ after cynarin introduction. Similarly, maximum probability of bindings reduced from 70% to 35% with a blocking effect of about 35% for a fixed contact time of 0.5 s or greater. Furthermore, average unbinding forces were reduced from 61.4 to 38.9 pN with a blocking effect of ~37% as compared with ~9% by SPR. AFM, which can provide accurate quantitative measures, is shown to be a good method for drug screening. The method could be applied to a wider variety of drug candidates with advances in bio-chip technology and a more comprehensive AFM database of protein-to-protein interactions.

Biotechnol. Bioeng. 2012;109: 2460–2467.

KEYWORDS: chip-based; protein–protein interaction; atomic force microscopy

Introduction

The immobilization of macromolecules such as proteins or DNA on solid substrates has been well researched (Caruso et al., 1997; Rusmini et al., 2007). Large molecules immobilized on silicon chips are called bio-chips. These included both protein and DNA chips with DNA microarray chips being well developed and widely used in the life sciences (Chan et al., 2011; Hoheisel, 2006; Mukherjee et al., 2004). DNA has a rigid structure and highly stable characteristics, making it very suitable for use as an immobilizer in bio-chips. Protein based bio-chips, however, have not progressed as far in their development due to some innate characteristics of protein that act as critical barriers to its development as an immobilizer such as homogeneity, orientation, folded–unfolded conformations, fragile 3D frames, etc. (Ramachandran et al., 2004; Templin et al., 2002). Choosing proper buffers and pH in protein solutions can overcome protein's conformational folding and unfolding problems. Both homogeneity and orientation may also be solved during engineering onto the chip. Furthermore, some specific proteins such as receptors have been found to have extremely small quantities of production. For example, many receptors have been purified and obtained within the range of micro grams. These may not be easily detected using conventional instruments but improved efficiency in using these scarce proteins is expected.

Immobilization of proteins on solid substrates such as silicon chips can be done either physically or by chemical reaction: (a) Physical adsorption on substrates occurs via non-covalent bonding such as van der Waals force, hydrogen bonding, hydrophobic, or electrostatic interaction. This method has some disadvantages such as non-uniformity of distribution, aggregation, etc. (Caruso et al., 1996). Loss of biological activity or the denaturation of adsorbed proteins on substrates is another drawback (Geddes et al., 1994; Zull et al., 1994); (b) Chemical reactions result in covalent bonding onto the substrate. One

Correspondence to: H.-M. Chen
Contract grant sponsor: National Applied Research Laboratories
Contract grant sponsor: National Nano Device Laboratories of Taiwan
Contract grant sponsor: National Science Council of Taiwan
Received 30 January 2012; Revision received 15 March 2012; Accepted 2 April 2012
Accepted manuscript online 17 April 2012;
Article first published online 26 April 2012 in Wiley Online Library (http://onlinelibrary.wiley.com/doi/10.1002/bit.24521/abstract)
DOI 10.1002/bit.24521

of the essential steps in immobilizing proteins on substrates is coupling among the functional groups at the surface coating; for example, the formation of highly ordered monolayers (self-assembled monolayer [SAM]) on silicon chips (Arya et al., 2007; Bhushan et al., 2005). The outwardly functional groups of SAM compounds, such as alkoxysilane amino groups, can be covalently coupled to protein with glutaraldehyde (Betancor et al., 2006; López-Gallego et al., 2005).

The importance of immobilization techniques and the use of atomic force microscopy (AFM) for evaluation of protein–protein (antigen–antibody) interactions have been previously applied (Hinterdorfer et al., 1996; Wang et al., 2011). In our previous works (Dong et al., 2006, 2009), we took, for example, the discovery of cynarin as an immunosuppressant. Cynarin (for its structure, see Fig. 1) was derived from *Echinacea purpurea* extract by after flowing through immobilized receptor (AFTIR) using selective binding to chip immobilized T-cell/CD28. CD28 is expressed by T-cells and is bound by B-cell/CD80 to trigger a costimulatory (Signal 2) T-cell response and the release by T-cells of IL-2 (Allison, 1994; June et al., 1990; Sharpe and Freeman, 2002). The comparative ability of cynarin to strongly bond with CD28 ahead of CD80 has been tested using surface plasma resonance (SPR). The results showed that cynarin bonds more strongly with CD28 than does CD80, making cynarin a potentially useful immunosuppressant agent. In this article, we use AFM measurement to see if it is a preferable method for measuring binding at the CD28 receptor site. We identify AFM as a useful tool for measuring the binding effect between T-cell/CD28 and B-cell/CD80. The results of this work will be useful in the development of new drug screening methods, including screening for immuno-suppression capabilities or other disease related agents.

Materials and Methods

Materials

[3-(2-Aminoethylamino)propyl] trimethoxysilane (3-APTMS) (99%), glutaraldehyde (25%), and bovine serum albumin (BSA) were obtained from Sigma–Aldrich (St. Louis, MO). Both CD28 and CD80 receptors were from ID Labs (London, ON, Canada). Cynarin was purchased from AppliChem (Darmstadt, Germany). Proteins with PBS buffer (pH 7.6) were prepared and the water used was deionized and distilled. Silicon-made tips for AFM (NanoWizard, JPK Instruments, Berlin, Germany) imaging and force measurement were ordered from Nanosensor (Neuchatel, Switzerland). Silicon wafers (6′) were purchased from Summit-Tech Resource Corp. (Hsinchu, Taiwan).

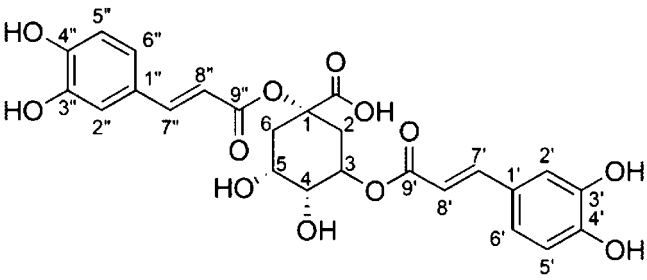

Figure 1. Structure of cynarin. The compound was identified by mass spectrometry and nuclear magnetic resonance spectroscopy (Dong et al., 2006).

Immobilization of Proteins on AFM Tip (afm-CD80) and Silicon Chip (imm-CD28)

The immobilization of proteins on the AFM tip (afm-CD80) and silicon oxide chip (imm-CD28) were similarly done: (i) For afm-CD80, AFM tips were cleaned in an oxygen plasma cleaner (PCD 150, Kaohsiung, Taiwan) under 250 mTorr and 80 W for 2 min and then immersed in piranha solution (H_2SO_4:H_2O_2 = 3:1, v/v) for 10 min to remove microparticles, metal ions, and organic materials. A SAM on the tips was formed by incubation with 3-APTMS (1%) in ethanol for 1 h. After washing the 3-APTMS-coated tips with ethanol/water several times, 2.5% glutaraldehyde (a common cross-linking protein) solution was added and the tips were incubated for 1 h. The unbounded glutaraldehyde was removed by rinsing with water. The treated tips were then inserted into CD80 solution (100 μg/mL) and incubated overnight at 4°C. (ii) For imm-CD28, a SiO_2 wafer was heated in a horizontal furnace to 1,050°C. After cutting the heated wafer into pieces, the 3-APTMS and glutaraldehyde steps in (i) above were similarly followed on the chips. The treated chips were then incubated with CD28 solution (25 μg/mL) for 30 min at room temperature. A 40 μg/mL BSA solution was applied to both treated tips (afm-CD80) and chips (imm-CD28) to fill-up the vacant space on their surfaces. Washing with NaOH (0.05 M) was performed before experiments.

Unbinding Force Measurements Between imm-CD28 and afm-CD80 by Atomic Force Microscopy

Current unbinding force (F_u) measurement via AFM between imm-CD28 and afm-CD80 can be empirically described as:

$$F_u = \left(\frac{k_B T}{x_\beta}\right) \ln\left(\frac{r x_\beta}{k_{off} k_B T}\right) \quad (1)$$

where k_B, T, x_β, r, and k_{off} indicate Boltzmann constant, absolute temperature (K), distance between energy potential minimum and energy barrier maximum, loading rate, and dissociation rate (off rate), respectively (Bell, 1978; Dufrêne and Hinterdorfer, 2008; Evans and Ritchie, 1997; Le Doan Thanh et al., 2011). The loading rate (r) can be defined as the

rate of force applied to the bond between proteins (e.g., r = pulling velocity × effective spring constant). Due to Equation (1), F_u is proportional to the logarithm of r. Therefore, selection of an optimum-loading rate for measurement of the unbinding forces among proteins may be essential (see "Unbinding Force Versus Loading Rate Section"). Moreover, the distance x_β can be assessed from the slope of the fitting line: for example,

$$x_\beta = \frac{k_B T}{\text{slope}} \tag{2}$$

with known x_β, the off rate (k_{off}) can be calculated from the intercept with the abscissa at zero force: for example,

$$k_{off} = r_{(F_u=0)} \frac{x_\beta}{k_B T} \tag{3}$$

Since the loading rate is related to the pulling velocity and tip spring constant, calibration of the AFM's tip spring constant (k) was necessary (in this work, k is about 0.0361 N/m by thermal noise measurement) (Hutter and Bechhoefer, 1993). Consequently, different pulling velocities varying from 5×10^{-8} to 2×10^{-5} m/s were applied in order to determine the relationship between the unbinding force and loading rate. Upon the loading rate being determined, F_u was measured for the interaction between afm-CD80 and imm-CD28 at >200 different locations. Furthermore, different contact times varying from 0 to 1 s were also applied (see "Unbinding Force Versus Contact Time Section") to obtain the optimum binding probability (BP_{max}). In this experiment, degradation during the measurement of unbinding force was not observed. To measure cynarin's ability to block interaction between imm-CD28 and afm-CD80, the following procedures were undertaken: (a) cynarin solution (500 μg/mL) was added to the imm-CD28 chips (30 min incubation). Afterward, the imm-CD28/cynarin chip was washed with PBS buffer; (b) the imm-CD28/cynarin chip was then examined using afm-CD80. Both the force curves and unbinding forces were recorded and calculated via the program provided by the manufacture.

Results

Roughness Measurement

Root mean square roughness (Rq) was used to observe the surface arrangement changes layer-by-layer in chips upon coating with different materials (Coen et al., 2001; Yang et al., 1999). Before coating, the original silicon oxide layer had an Rq of about 296 ± 6 pm based on the measurement of a $500 \times 500\ nm^2$ area on the chips. After coating with 3-APTMS and glutaraldehyde, the Rqs were about 272 ± 3 and 252 ± 15 pm, respectively. Upon the addition of CD28 (imm-CD28), the Rq was about 600 ± 6 pm. Figure 2A shows that the peak height and width of CD28 were about 2 and 19 nm, respectively (see the red arrows, height and width are not of the same scale). After the addition of afm-CD80 to imm-CD28, Rq increased to about 1,064 ± 39 pm and height to about 4 nm (see red arrow below Fig. 2B). The lower Rq of on-chip imm-CD28 may indicate that the homogeneity of the protein distribution on the chip is high (i.e., protein aggregation is not apparent). The higher Rq after the addition of afm-CD80 may imply that binding among these proteins was not completely orderly, including single/multiple bindings and with/without right orientation of proteins. However, if cynarin was added to imm-CD28 (i.e., imm-CD28 + cynarin) before the addition of afm-CD80, Rq was about 570 ± 19 pm. After the addition of afm-CD80 (i.e., imm-CD28 + cynarin + afm-CD80), the Rq changed to about 554 ± 8 pm. The final height was about 1.5 nm (see the red arrow of Fig. 2C) as compared with that of 4 nm without the addition of cynarin.

Unbinding Force Versus Loading Rate

Based on Equation (1), one can predict that the relationship between the unbinding force and logarithm of the loading rate is linear; however, there may exist some anomalous factors such as the phenomena of multiple inner and outer barriers (Berquand et al., 2005; de Odrowaz Piramowicz et al., 2006; Merkel et al., 1999), which could interfere with the results. Our experimental observations showed that unbinding forces between imm-CD28 and afm-CD80 are best described (most probably) as linearly increasing with the logarithm of loading rates (Fig. 3) under a fixed contact time of 0.5 s (for contact times used, see below). There are two distinct linear sections shown in the plot (blue and red dots of Fig. 3), the breaking point (bp) for these two sections is at a loading rate of about 1×10^5 pN/s. If the loading rates are smaller than bp, both x_β and k_{off} are 0.78 nm and 1.2 s^{-1}, respectively (calculations due to Eqs. 2 and 3) as compared with 0.12 nm and $7.1 \times 10^2\ s^{-1}$, respectively if the loading rates are larger than the bp.

Unbinding Force Versus Contact Time

Contact time used between the two proteins (imm-CD28 and afm-CD8) may affect the accuracy of unbinding force measurement, especially for comparisons between before and after the addition of cynarin. Figure 4 shows the results between binding probability and contact time under the conditions of "without" (imm-CD28/afm-CD80; in blue) and "with" cynarin (imm-CD28/cynarin/afm-CD80; in red). With increasing contact time between afm-CD80 and imm-CD28, the binding probability increases and reaches a steady maximum equal or larger than 0.5 s (see Fig. 4 in blue). The same tendency appears in the case of "blocking" by cynarin (see Fig. 4 in red). Both maximum binding probability (BP_{max}) of "without" and "with" the blocking factor were about 70% and 35%, respectively (e.g.,

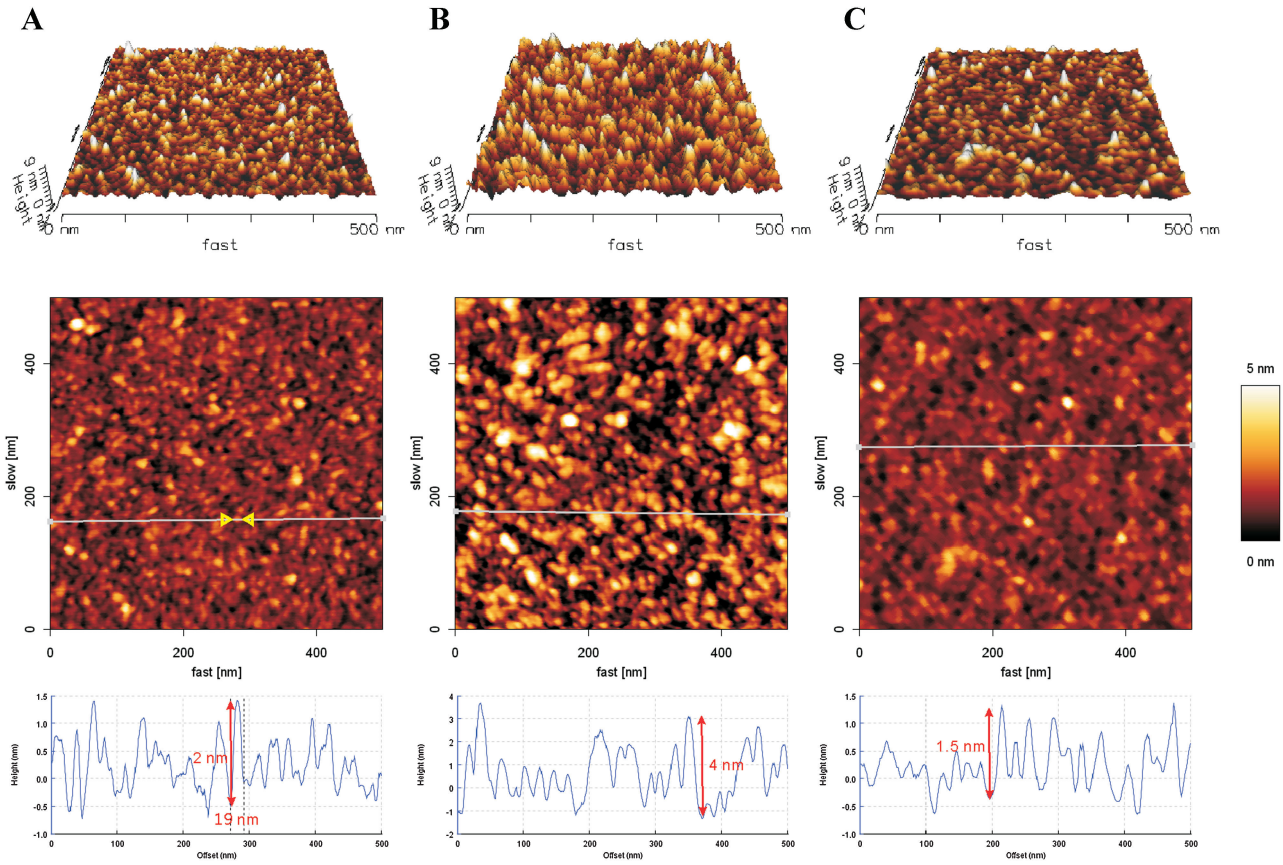

Figure 2. Top 1st and 2nd row figures are 3D and 2D topographies, respectively, of AFM images: (**A**) imm-CD28 on SiO_2 chip; (**B**) afm-CD80 to imm-CD28; and (**C**) afm-CD80 to imm-CD28/cynarin. Bottom figures give corresponding chip surface cross-sections (indicated by red arrows) for height (nm) versus offset (nm).

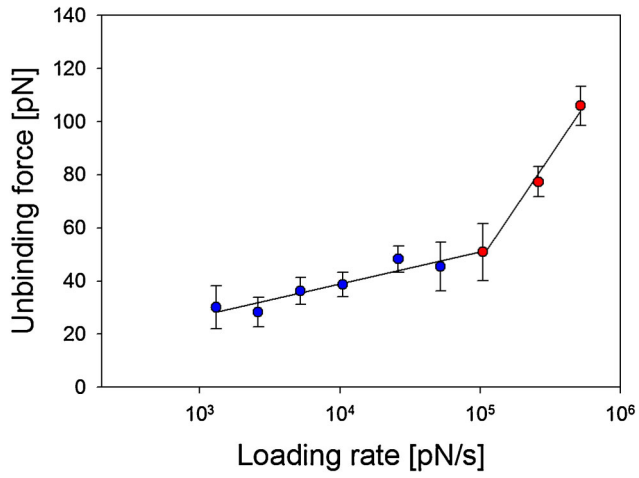

Figure 3. Unbinding force versus loading rate. Two linear sections (blue and red dots) were obtained with a breaking point at 1×10^5 pN/s.

$\Delta BP_{max} = -35\%$). The results imply that accurate measurement of the blocking effect or protein-to-protein interaction may be done at a contact time equal to or beyond 0.5 s.

Blocking Effect

Results of unbinding force measurements of imm-CD28 versus afm-CD80 and imm-CD28/cynarin versus afm-CD80 with a loading rate of 1.44×10^4 pN/s and contact time of 0.5 s are shown in Figure 5A and B, respectively. Non-apparent unbinding forces below 30 pN were considered as noise and non-specific binding. In Figure 5A, a larger part distribution of higher unbinding forces is observed due to multiple imm-CD28/afm-CD80 bindings. With the addition of cynarin, however, a larger part distribution of lower unbinding forces is obtained (see Fig. 5B). If the apparent bindings (binding events) including single and multiple bonds are counted, the probability of binding events for imm-CD28/afm-CD80 is about $61 \pm 5\%$. However, with the addition of cynarin, the binding events reduce to about $47 \pm 6\%$. The average unbinding force of imm-CD28/afm-CD80 is about 61.4 pN. After blocking by cynarin, the

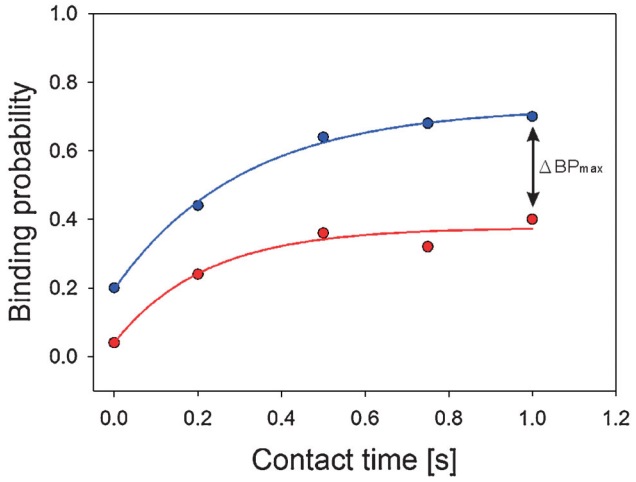

Figure 4. Measurements of binding probability with different contact times. The contact times of tip afm-CD80 to the chip surface of imm-CD28 were established and the binding probabilities measured without (in blue) and with (in red) the addition of cynarin. The blocking effect was obviously observed with significant difference in ΔBP_{max}.

average unbinding force is reduced to about 38.9 pN (unbinding forces above 250 pN are not counted). Accordingly, the blocking effect between imm-CD28 and afm-CD80 by cynarin is about 37%.

Discussion

Immobilization of proteins (including extracelluar domain of transmembrane protein like CD28 used in this work) on chip by covalent binding with coupling compound(s) such as glutaraldehyde (Betancor et al., 2006; López-Gallego et al., 2005) or 1-ethyl-3-(dimethyl-aminopropyl) carbodi-imide hydrochloride (EDC)/*N*-hydroxysulpho-succinimide (NHS) (Johnsson et al., 1991) has been widely applied in protein chip preparation. Since the chip was treated in buffer solution under physiological condition during the experiment, protein structure can be maintained in its folded form. Successful examples were shown in our previous reports by using CD28 immobilized on chip for binding experiment with CD80 via surface plasma resonance (SPR) measurements (Dong et al., 2006, 2009). Instead of whole live-cell (Duman et al., 2010), using isolated proteins is an intention to establish an easy, fast and reliable drug screening system. In this communication, we confirmed that the drug screening (e.g., CD28 can be blocked from CD80 by small molecule like cynarin) can be done by AFM (direct binding measurement), instead of SPR (indirect binding measurement).

For a new drug screening system to be established based on the current set-up of chip-based protein–protein interactions using AFM as a detection tool, some detailed analysis needs to be done. For protein–protein interaction

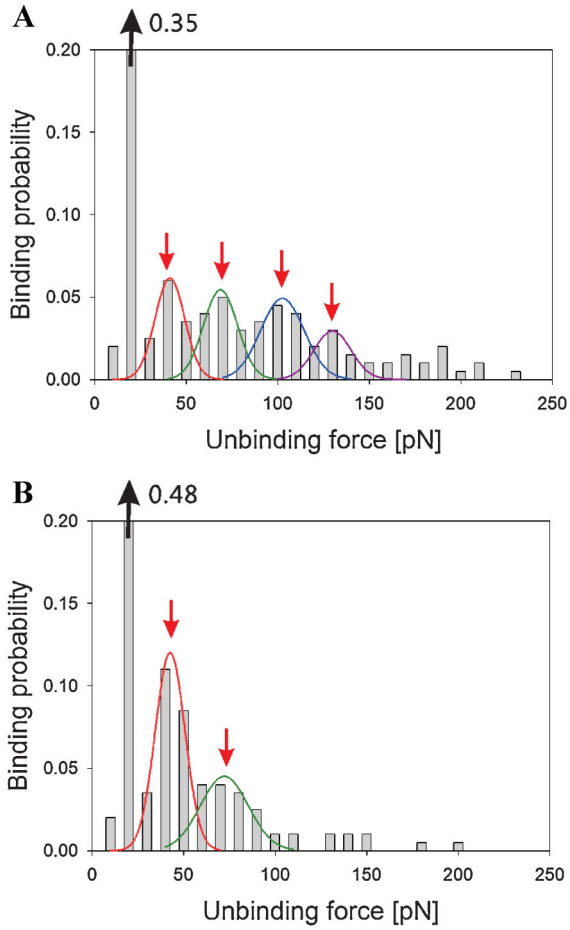

Figure 5. **A**: Distribution of unbinding forces between imm-CD28/afm-CD80. **B**: Distribution of unbinding forces with the addition of cynarin to imm-CD28 before afm-CD80. Red arrows indicate the most probable unbinding forces of multi-imm-CD28/afm-CD80 complexes. A higher binding probability with lower unbinding forces is observed in the case of the addition of cynarin into imm-CD28.

on the silicon chip surface, we have observed that the Rq became smaller after coating with 3-APTMS and glutaraldehyde (from 296 ± 6 to 272 ± 6 pm and 252 ± 15 pm, respectively). This indicates that the chip surface was smoother after the SAM material was coated. Both smaller size and one monolayer coating may be the reasons. Beyond this level, the Rq is observed to be higher with the addition of CD28 (600 ± 6 pm). Although immobilization exists on the silicon dioxide substrate via amine–amine cross-linking between glutaraldehyde and CD28, smoothness was not as good as the SAM surface alone. Consequently, after the binding of CD80 to imm-CD28, Rq was expected to be higher ($1{,}064 \pm 39$ pm). When CD80 binds with CD28, the AFM image shows a higher peak of 4 nm than that of 2 nm for CD28 alone (Fig. 2) and Rq increases dramatically to 1,064 pm. This means that CD80 bound specifically to CD28 and the resultant CD28/CD80 complex leads to a higher peak and roughness score. Although these complexes seem not to be orderly on the chip surface, both bioactivity

(immuno-response) and specific binding (receptor and ligand) can be obtained. With the addition of cynarin to CD28 (before CD80), the Rq of CD28–cynarin complex on the chip surface does not decrease much. This may be because cynarin is a small molecule (516.45 MW) and the cynarin/CD28 complex does not change the surface topography much. As CD80 is introduced, Rq is similar to that of the cynarin/CD28 complex result, meaning binding between CD28 and CD80 is unlikely to have occurred. This important result proves CD80 blocking by cynarin.

Furthermore, we observed that unbinding between imm-CD28 and afm-CD80 was more stable at a lower loading rate. In Figure 3, two different slopes appeared between the unbinding force and loading rate, which may imply that dissociation of the molecular complex involves more than one activation barrier. When a large force is applied, the energy profile likely changes a lot and the outer barrier may be suppressed by this force, resulting in inner barrier dominating the kinetic relationship (Merkel et al., 1999). If the loading rate is smaller than 1×10^5 pN/s, the dissociation rate of this complex is smaller ($\sim 1.2\ s^{-1}$, which is similar to previously reported data $\sim 1.6\ s^{-1}$ by SPR measurements (van der Merwe et al., 1997) and the lifetime longer (~ 0.83 s as compared with $\sim 1.4 \times 10^{-3}$ s if the loading rate $> 1 \times 10^5$ pN/s). In this work, a high loading rate is, therefore, not used because of abrupt changes may occur leading to larger variations in measurement. Consequently, a loading rate of about 1.44×10^4 pN/s was applied. The above quantitative analysis may be a necessary procedural step to ensure the accuracy of chip-based protein–protein drug screening methods in future studies.

The blocking effect of cynarin to CD28 has been shown by our previous reports using SPR measurement (Dong et al., 2006, 2009). In this article, we are able to confirm this result using on-chip protein immobilization and the AFM technique. For imm-CD28 and afm-CD80 binding measurements, larger unbinding forces with multiple bonds (Fig. 5A, red arrows) were observe compared to imm-CD28 + cynarin before the addition of afm-CD80 (Fig. 5B, red arrows). As noted, afm-CD80 proteins bound with imm-CD28 through either single or multiple bonding with the latter case leading to larger unbinding forces (Zhang and Moy, 2003). Theoretically, protein diameter (d) can be estimated from AFM images using the formula: $d = W^2/8R$, where R is the tip's radius of curvature and W is the width of the protein (as per AFM manufacture's handbook, NanoWizard Handbook Version 1.3, page 30, JPK instruments). Based on Figure 2A, the diameter (d) of imm-CD28 was calculated to be about 4.5 nm, where $R = 10$ nm and $W = 19$ nm. The difference between the estimated diameter (4.5 nm) and height (2 nm; see Fig. 2A) may reflect the fixing of one side of the protein on the chip's surface, resulting in the protein not being truly spherical. Similarly, imm-CD80 was estimated to be 6 nm in diameter but with a 3 nm height (AFM image not shown). The difference between diameter and height was again obtained for CD80. Under the known sizes of proteins shown above, it's possible to estimate how many CD80 molecules immobilized on the AFM's tip interact with CD28 molecules immobilized on the chip. When the AFM tip approaches the chip's surface, only a few molecules at the tip can possibly react with CD28 molecules. This is termed the effective region of the tip (see Fig. 6). Figure 6 gives a schematic representation under the following assumptions: (i) the effective region is a spherical crown; (ii) CD80 molecules are nearly spherical; (iii) proteins are incompressible during reactions; (iv) the longest reaction distance is set to 4 nm based on the measurements shown in Figure 2, where the CD80/CD28 complex has a height of ~ 4 nm. Given these assumptions, the maximum height (H) of the effective region is 1 nm (see Fig. 6) with the extended height being 3 nm. The total effective area on the tip is about 62 nm^2, which covers a region occupied by about nine CD80 molecules. Our experimental results indicate only four CD28/CD80 complexes being formed at the effective area; the difference between the theoretical result of ~ 9 potential bonds and the 4 achieved may be due to non-appropriate protein orientation, leading to fewer successful bonds.

Based on the above, two potential cases exist for the unbinding forces of the protein bonds: (i) single bonding whereby the unbinding force is about 41.1 pN based on fitting with the Gaussian peak; and (ii) multiple bonding whereby the unbinding forces are increased from 68.7 and 101.7 to about 129.9 pN (see Fig. 5A). After cynarin blocking, it would be expected that non-specific bindings would increase and there would be a reduction in the most probable bindings between imm-CD28 and afm-CD80. The experimental results show that only two peaks (42.6 and 72.2 pN) were observed (Fig. 5B, red arrows). This indicates that the number of imm-CD28 molecules binding with afm-CD80 was reduced presumably by the blocking action of cynarin molecules such that the overall binding force was reduced. Calculating the average unbinding force shows a reduction from 61.4 to 38.9 pN ($\Delta = -22.5$ pN or

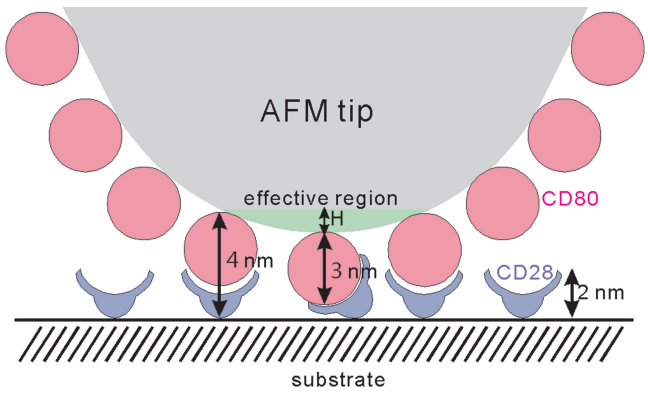

Figure 6. Effective interactions between CD80 and CD28 molecules. Only CD80 molecules located in the effective region (green area) can bond with CD28 molecules of the substrate.

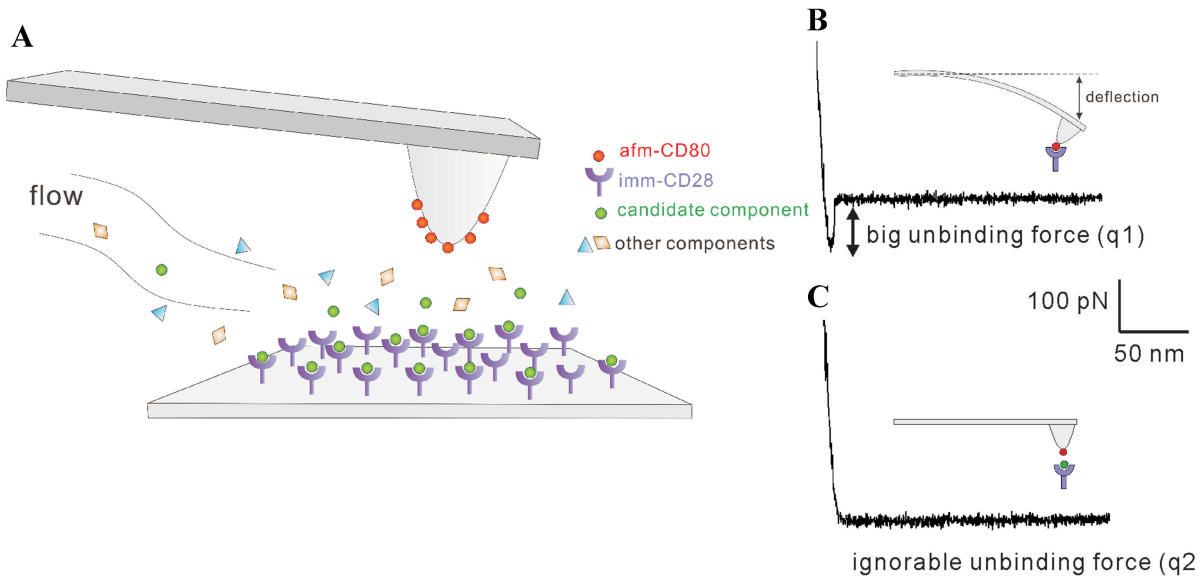

Figure 7. Schematic of new AFM drug screening technique: (**A**) Schematic of AFM method for drug screening immunosuppressant candidate *Echinacea purpurea* derived cynarin. Method allows for quantitative investigation of blocking action by cynarin between T-cell/CD28 and B-cell/CD80 using the following measures: (**B**) "Without" blocking effect, large adhesion force (q_1) obtained between afm-CD80 and imm-CD28, and (**C**) "With" blocking effect, negligible binding force (q_2) between afm-CD80 and imm-CD28. Significant difference $\Delta = q_1 - q_2$ quantitatively measures effectiveness of blocking action and the method can be used to easily identify drug candidates from complex extracts.

about 36.7% reduction). If we estimate the probability of binding events for both non-blocking and blocking, we can see a change from 61% to 47% ($\Delta = -14\%$ or about a 23% reduction). Furthermore, the maximum probability of bindings is reduced to about 40% after cynarin blocking, regardless of the contact times used (see Fig. 4). The above results for average unbinding force, maximum probability and contact times are all strongly indicative of the effectiveness of cynarin as a blocking agent and potential immunosuppressant and the success of the AFM technique.

Figure 7 gives a schematic representation of the AFM method for the case of *E. purpurea* derived cynarin drug screening. Cynarin is shown by this method to be a strong candidate for development in the reduction of allergic reactions by blocking the active site T-cell/CD28 for costimulatory (Signal 2) T-cell response and the release of T-cell IL-2. In the case of "without" blocking, a large adhesion force (q_1) was obtained between afm-CD80 and imm-CD28. However, for the "with" blocking by cynarin case, only a negligible unbinding force (q_2) between afm-CD80 and imm-CD28 was obtained. The significant difference can be quantitatively given by $\Delta = q_1 - q_2$. All other components with non-significant bindings (small Δ) should be excluded.

Conclusions

This study looks at the use of AFM as a potential method for screening drug candidates. The technique is applied to the known immunosuppressant candidate *E. purpurea* derived cynarin. Cynarin binds with T-cell/CD28 to block B-cell/CD80 and prevent costimulatory T-cell response. The method showed an easily detectable significant difference in unbinding force between afm-CD80 and imm-CD28 before and after the introduction of cynarin. The method allows for a quantitative measure of this difference and therefore should be a favored technique as a drug screening method. With continued advancements in microarrays and the development of a mature AFM statistical database, this drug screening method could be applied to a wide variety of drug candidates.

This work was in part supported by National Applied Research Laboratories, National Nano Device Laboratories of Taiwan and in part by National Science Council of Taiwan.

References

Allison JP. 1994. CD28-B7 interactions in T-cell activation. Curr Opin Immunol 6(3):414–419.

Arya SK, Prusty AK, Singh SP, Solanki PR, Pandey MK, Datta M, Malhotra BD. 2007. Cholesterol biosensor based on N-(2-aminoethyl)-3-aminopropyl-trimethoxysilane self-assembled monolayer. Anal Biochem 363(2):210–218.

Bell GI. 1978. Models for the specific adhesion of cells to cells. Science 200(4342):618–627.

Berquand A, Xia N, Castner DG, Clare BH, Abbott NL, Dupres V, Adriaensen Y, Dufrene YF. 2005. Antigen binding forces of single antilysozyme Fv fragments explored by atomic force microscopy. Langmuir 21(12):5517–5523.

Betancor L, López-Gallego F, Hidalgo A, Alonso-Morales N, Mateo GD-OC, Fernández-Lafuente R, Guisán JM. 2006. Different mechanisms of protein immobilization on glutaraldehyde activated supports: Effect of

support activation and immobilization conditions. Enzyme Microb Technol 39(4):877–882.
Bhushan B, Tokachichu DR, Keener MT, Lee SC. 2005. Morphology and adhesion of biomolecules on silicon based surfaces. Acta Biomater 1(3):327–341.
Caruso F, Rodda E, Furlong DN. 1996. Orientational aspects of antibody immobilization and immunological activity on quartz crystal microbalance electrodes. J Colloid Interface Sci 178(1):104–115.
Caruso F, Rodda E, Furlong DN, Niikura K, Okahata Y. 1997. Quartz crystal microbalance study of DNA immobilization and hybridization for nucleic acid sensor development. Anal Chem 69(11):2043–2049.
Chan M-L, Jaramillo G, Hristova KR, Horsley DA. 2011. Magnetic scanometric DNA microarray detection of methyl tertiary butyl ether degrading bacteria for environmental monitoring. Biosensors Bioelectron 26(5):2060–2066.
Coen MC, Lehmann R, Gröning P, Bielmann M, Galli C, Schlapbach L. 2001. Adsorption and bioactivity of protein A on silicon surfaces studied by AFM and XPS. J Colloid Interface Sci 233(2):180–189.
de Odrowaz Piramowicz M, Czuba P, Targosz M, Burda K, Szymonski M. 2006. Dynamic force measurements of avidin–biotin and streptavdin–biotin interactions using AFM. Acta Biochim Pol 53(1):93–100.
Dong GC, Chuang PH, Forrest MD, Lin YC, Chen HM. 2006. Immunosuppressive effect of blocking the CD28 signaling pathway in T-cells by an active component of *Echinacea* found by a novel pharmaceutical screening method. J Med Chem 49(6):1845–1854.
Dong G-C, Chuang P-H, Chang K-C, Jan P-S, Hwang P-I, Wu H-B, Yi M, Zhou H-X, Chen H. 2009. Blocking effect of an immuno-suppressive agent, cynarin, on CD28 of T-Cell receptor. Pharm Res 26(2):375–381.
Dufrêne Y, Hinterdorfer P. 2008. Recent progress in AFM molecular recognition studies. Pflügers Archiv Eur J Physiol 456(1):237–245.
Duman M, Pfleger M, Zhu R, Rankl C, Chtcheglova LA, Neundlinger I, Bozna BL, Mayer B, Salio M, Shepherd D, Polzella P, Moertelmaier M, Kada G, Ebner A, Dieudonne M, Schutz GJ, Cerundolo V, Kienberger F, Hinterdorfer P. 2010. Improved localization of cellular membrane receptors using combined fluorescence microscopy and simultaneous topography and recognition imaging. Nanotechnology 21(11):115504.
Evans E, Ritchie K. 1997. Dynamic strength of molecular adhesion bonds. Biophys J 72(4):1541–1555.
Geddes NJ, Martin AS, Caruso F, Urquhart RS, Furlong DN, Sambles JR, Than KA, Edgar JA. 1994. Immobilisation of IgG onto gold surfaces and its interaction with anti-IgG studied by surface plasmon resonance. J Immunol Methods 175(2):149–160.
Hinterdorfer P, Baumgartner W, Gruber HJ, Schilcher K, Schindler H. 1996. Detection and localization of individual antibody–antigen recognition events by atomic force microscopy. Proc Natl Acad Sci 93(8):3477–3481.
Hoheisel JD. 2006. Microarray technology: Beyond transcript profiling and genotype analysis. Nat Rev Genet 7(3):200–210.
Hutter JL, Bechhoefer J. 1993. Calibration of atomic force microscope tips. Rev Sci Instrum 64(7):1868–1873.
Johnsson B, Löfås S, Lindquist G. 1991. Immobilization of proteins to a carboxymethyldextran-modified gold surface for biospecific interaction analysis in surface plasmon resonance sensors. Anal Biochem 198(2):268–277.
June CH, Ledbetter JA, Linsley PS, Thompson CB. 1990. Role of the CD28 receptor in T-cell activation. Immunol Today 11:211–216.
Le Doan Thanh L, Guérardel Y, Loubière P, Mercier-Bonin M, Dague E. 2011. Measuring kinetic dissociation/association constants between *Lactococcus lactis* bacteria and mucins using living cell probes. Biophys J 101(11):2843–2853.
López-Gallego F, Betancor L, Mateo C, Hidalgo A, Alonso-Morales N, Dellamora-Ortiz G, Guisán JM, Fernández-Lafuente R. 2005. Enzyme stabilization by glutaraldehyde crosslinking of adsorbed proteins on aminated supports. J Biotechnol 119(1):70–75.
Merkel R, Nassoy P, Leung A, Ritchie K, Evans E. 1999. Energy landscapes of receptor–ligand bonds explored with dynamic force spectroscopy. Nature 397(6714):50–53.
Mukherjee S, Berger MF, Jona G, Wang XS, Muzzey D, Snyder M, Young RA, Bulyk ML. 2004. Rapid analysis of the DNA-binding specificities of transcription factors with DNA microarrays. Nat Genet 36(12):1331–1339.
Ramachandran N, Hainsworth E, Bhullar B, Eisenstein S, Rosen B, Lau AY, Walter JC, LaBaer J. 2004. Self-assembling protein microarrays. Science 305(5680):86–90.
Rusmini F, Zhong Z, Feijen J. 2007. Protein Immobilization strategies for protein biochips. Biomacromolecules 8(6):1775–1789.
Sharpe AH, Freeman GJ. 2002. The B7-CD28 superfamily. Nat Rev Immunol 2(2):116–126.
Templin MF, Stoll D, Schrenk M, Traub PC, Vöhringer CF, Joos TO. 2002. Protein microarray technology. Trends Biotechnol 20(4):160–166.
van der Merwe PA, Bodian DL, Daenke S, Linsley P, Davis SJ. 1997. CD80 (B7-1) binds both CD28 and CTLA-4 with a low affinity and very fast kinetics. J Exp Med 185(3):393–403.
Wang C, Wang J, Deng L. 2011. Evaluating interaction forces between BSA and rabbit anti-BSA in sulphathiazole sodium, tylosin and levofloxacin solution by AFM. Nanoscale Res Lett 6(1):579.
Yang Z, Galloway JA, Yu H. 1999. Protein interactions with poly(ethylene glycol) self-assembled monolayers on glass substrates: Diffusion and adsorption. Langmuir 15(24):8405–8411.
Zhang X, Moy VT. 2003. Cooperative adhesion of ligand-receptor bonds. Biophys Chem 104(1):271–278.
Zull JE, Reed-Mundell J, Lee YW, Vezenov D, Ziats NP, Anderson JM, Sukenik CN. 1994. Problems and approaches in covalent attachment of peptides and proteins to inorganic surfaces for biosensor applications. J Indus Microbiol Biotechnol 13(3):137–143.